TABLE 3 Factors influencing functional outcome according to the Wexner score

Univariate analysis	*n*	Median Wexner score	*p* Value
Preoperative radiotherapy			0.01
Yes	27	10	
No	77	8	
Sex			0.019
Male	76	9	
Female	28	6.5	
Age			0.707
≦65 years	78	8	
>65 years	26	9	
Type of surgery			0.654
Total ISR	26	9	
Subtotal ISR and partial ISR	78	8	
PESR			0.953
PESR	16	9	
ISR	88	8.5	
Tumor category			0.401
T1–T2	29	8	
T3–T4	75	9	
Distance from anal verge			0.649
<4 cm	42	9	
≧4 cm	62	8	

Multivariate analysis (multiple linear regression model)

	Coefficient (β)	SE	95 % CI	*p* Value
Intercept	16.087	2.161		
Preoperative CRT	−2.553	1.042	−4.620 to −0.486	0.016
Sex	−2.076	1.030	−4.119 to −0.033	0.046

PESR group, patients showed a higher positive CRM rate (36.7 %). Quirke et al.[22] reported CRM involvement as a key factor in rectal cancer treatment. The positive CRM group in this study showed worse prognosis. Additional therapy (radiation and abdominoperineal resection) should be considered in the positive CRM group, although no patient in this study received such treatment.

The next question to be answered concerns long-term functional and QOL outcomes. This operation involves side effects of internal sphincter resection or PESR. In our study, 70 % of patients showed good continence (Wexner score ≤10) at >5 years, although fragmentation, gas incontinence, and soiling were still experienced. The operative type of ISR did not matter for the long-term functional outcomes, as shown in other reports.[7,17] However, significant differences in continence were evident between male and female patients and between CRT and surgery groups. In particular, preoperative CRT was a strong predictor of incontinence in both univariate and multivariate analyses. Similar results have been reported in our own and other previous reports.[7,25] However, Denost et al.[17] reported that the risk of fecal incontinence after ISR depended on tumor level and height of the anastomosis. Various factors including cultural and social factors may exert influences on anal function. In our experience, postoperative anal function was decreased when CRT was very effective in patients undergoing ISR. One reason for worsened anal function may be marked neural degeneration caused by preoperative CRT.[26] However, we cannot definitively answer why postoperative anal function was better in female patients.

According to a QOL study by Sprangers et al.[27] patients with a permanent stoma experienced greater restrictions to level of social function than patients with ultralow resection. Conversely, Renner et al.[28] reported no differences in SF-36 scores between patients with coloanal anastomosis and those with anterior resection. In the present study, patients after ISR with or without PESR showed PCS and MCS at >5 years equal to or better than those preoperatively. Our results show that general QOL is acceptable in patients treated by ISR. The most popular scale used for measuring patient perception of fecal incontinence is the fecal incontinence QOL scale.[29] We demonstrated that mFIQL offers satisfactory psychometric reliability and validity for assessing the psychosocial dimension of QOL among patients after ISR.[20] The CRT group showed significantly worse mFIQL scores than the surgery group after long-term follow-up. This suggests that more functional problems might be associated with fecal incontinence in the CRT group. Therefore, new neoadjuvant therapies without radiation as an alternative to CRT may be necessary for obtaining better function and QOL, although CRT offers better local control. These results came from our single-center study, and comparative series involving multiple centers would be more useful for assessing function and QOL.

In conclusion, ISR with negative CRM represents a feasible surgical option in terms of oncologic outcomes for patients with very low rectal cancer at long-term follow-up. Long-term results for postoperative anal function and QOL are also acceptable in the majority of patients, although CRT is associated with disturbance.

ACKNOWLEDGMENT This study was supported in part by a Grant-in-Aid from the National Cancer Center (NCC) Research and Development Fund (23-A-26) in Japan.

CONFLICT OF INTEREST The authors declare no conflicts of interest.

REFERENCES

1. Heald RJ, Ryall RD. Recurrence and survival after total mesorectal excision for rectal cancer. *Lancet.* 1986;1:1479–82.
2. Schiessel R, Karner-Hanusch J, Herbst F, et al. Intersphincteric resection for low rectal tumours. *Br J Surg.* 1994;81:1376–8.
3. Bannon JP, Marks GJ, Mohiuddin M, et al. Radical and local excisional methods of sphincter-sparing surgery after high-dose radiation for cancer of the distal 3 cm of the rectum. *Ann Surg Oncol.* 1995;2:221–7.
4. Braun J, Treutner KH, Winkeltau G, et al. Results of intersphincteric resection of the rectum with direct coloanal anastomosis for rectal carcinoma. *Am J Surg.* 1992;163:407–12.
5. Rullier E, Laurent C, Bretagnol F, et al. Sphincter-saving resection for all rectal carcinomas: the end of the 2-cm distal rule. *Ann Surg.* 2005;241:465–9.
6. Saito N, Moriya Y, Shirouzu K, et al. Intersphincteric resection in patients with very low rectal cancer: a review of the Japanese experience. *Dis Colon Rectum.* 2006;49(10 Suppl.):S13–22.
7. Chamlou R, Parc Y, Simon T, et al. Long-term results of intersphincteric resection for low rectal cancer. *Ann Surg.* 2007;246:916–21.
8. Akasu T, Takawa M, Yamamoto S, et al. Intersphincteric resection for very low rectal adenocarcinoma: univariate and multivariate analyses of risk factors for recurrence. *Ann Surg Oncol.* 2008;15:2668–76.
9. Schiessel R, Novi G, Holzer B, et al. Technique and long-term results of intersphincteric resection for low rectal cancer. *Dis Colon Rectum.* 2005;48:1858–65.
10. Hohenberger W, Merkel S, Matzel K, et al. The influence of abdomino-peranal (intersphincteric) resection of lower third rectal carcinoma on the rates of sphincter preservation and locoregional recurrence. *Colorectal Dis.* 2006;8:23–33.
11. Yamada K, Ogata S, Saiki Y, et al. Long-term results of intersphincteric resection for low rectal cancer. *Dis Colon Rectum.* 2009;52:1065–71.
12. Saito N, Sugito M, Ito M, et al. Oncologic outcome of intersphincteric resection for very low rectal cancer. *World J Surg.* 2009;33:1750–6.
13. Weiser MR, Quah HM, Shia J, et al. Sphincter preservation in low rectal cancer is facilitated by preoperative chemoradiation and intersphincteric dissection. *Ann Surg.* 2009;249:236–42.
14. Krand O, Yalti T, Tellioglu G, et al. Use of smooth muscle plasty after intersphincteric rectal resection to replace a partially resected internal anal sphincter: long-term follow-up. *Dis Colon Rectum.* 2009;52:1895–901.
15. Jorge JM, Wexner SD. Etiology and management of fecal incontinence. *Dis Colon Rectum.* 1993;36:77–97.
16. Sobin LH, Wittekind Ch. International Union Against Cancer TMN classification of malignant tumours, 6th ed. New York: Wiley-Liss; 2002.
17. Denost Q, Laurent C, Capdepont MCRA, et al. Risk factors for fecal incontinence after intersphincteric resection for rectal cancer. *Dis Colon Rectum.* 2011;54:963–8.
18. Hashimoto H, Green J, Iwao Y, et al. Reliability, validity, and responsiveness of the Japanese version of the Inflammatory Bowel Disease Questionnaire. *J Gastroenterol.* 2003;38:1138–43.
19. Fukuhara S, Bito S, Green J, et al. Translation, adaptation, and validation of the SF-36 Health Survey for use in Japan. *J Clin Epidemiol.* 1998;51:1037–44.
20. Hashimoto H, Shiokawa H, Funahashi K, et al. Development and validation of a modified fecal incontinence quality of life scale for Japanese patients after intersphincteric resection for very low rectal cancer. *J Gastroenterol.* 2010;45:928–35.
21. Nagtegaal ID, Quirke P. What is the role for the circumferential margin in the modern treatment of rectal cancer? *J Clin Oncol.* 2008;26:303–12.
22. Quirke P, Steele R, Monson J, et al. Effect of the plane of surgery achieved on local recurrence in patients with operable rectal cancer: a prospective study using data from the MRC CR07 and NCIC-CTG CO16 randomised clinical trial. *Lancet.* 2009;373:821–28.
23. Taylor FGM, Quirke P, Heald RJ, et al. One millimetre is the safe cut-off for magnetic resonance imaging prediction of surgical margin status in rectal cancer. *Br J Surg.* 2011;98:872–9.
24. Martin ST, Heneghan HM, Winter DC. Systematic review of outcomes after intersphincteric resection for low rectal cancer. *Br J Surg.* 2012;99:603–12.
25. Ito M, Saito N, Sugito M, et al. Analysis of clinical factors associated with anal function after intersphincteric resection for very low rectal cancer. *Dis Colon Rectum.* 2009;52:64–70.
26. Nishizawa Y, Fujii S, Saito N, et al. The association between anal function and neural degeneration after preoperative chemoradiotherapy followed by intersphincteric resection. *Dis Colon Rectum.* 2011;54:1423–9.
27. Sprangers MA, Taal BG, Aaronson NK, et al. Quality of life in colorectal cancer. Stoma vs. nonstoma patients. *Dis Colon Rectum.* 1995;38:361–9.
28. Renner K, Rosen HR, Novi G, et al. Quality of life after surgery for rectal cancer: do we still need a permanent colostomy? *Dis Colon Rectum.* 1999;42:1160–7.
29. Rockwood TH, Church JM, Fleshman JW, et al. Fecal incontinence quality of life scale: quality of life instrument for patients with fecal incontinence. *Dis Colon Rectum.* 2000;43:9–16.

OPEN ACCESS Freely available online

PLOS | ONE

Hypoxia Imaging Endoscopy Equipped with Laser Light Source from Preclinical Live Animal Study to First-In-Human Subject Research

Kazuhiro Kaneko[1,2]*, Hiroshi Yamaguchi[3]*, Takaaki Saito[3], Tomonori Yano[1], Yasuhiro Oono[1], Hiroaki Ikematsu[1], Shogo Nomura[4], Akihiro Sato[4], Motohiro Kojima[5], Hiroyasu Esumi[6], Atsushi Ochiai[5]

1 Department of Gastroenterology, Endoscopy Division, National Cancer Center Hospital East, Kashiwa, Chiba, Japan, **2** Division of Science and Technology for Endoscopy and Surgery, National Cancer Center Hospital East, Kashiwa, Chiba, Japan, **3** Imaging Technology Center, FUJIFILM Corporation, Kaisei, Kanagawa, Japan, **4** Clinical Trial Section, National Cancer Center, Kashiwa, Chiba, Japan, **5** Department of Pathology, National Cancer Center Hospital East, Kashiwa, Chiba, Japan, **6** Research Institute for Biomedical Sciences, Tokyo University of Science, Noda, Chiba, Japan

Abstract

A goal in next-generation endoscopy is to develop functional imaging techniques to open up new opportunities for cancer diagnosis. Although spatial and temporal information on hypoxia is crucial for understanding cancer physiology and expected to be useful for cancer diagnosis, existing techniques using fluorescent indicators have limitations due to low spatial resolution and invasive administration. To overcome these problems, we developed an imaging technology based on hemoglobin oxygen saturation in both the tumor and surrounding mucosa using a laser endoscope system, and conducted the first human subject research for patients with aero-digestive tract cancer. The oxygen saturation map overlapped the images of cancerous lesions and indicated highly heterogeneous features of oxygen supply in the tumor. The hypoxic region of the tumor surface was found in both early cancer and cancer precursors. This technology illustrates a novel aspect of cancer biology as a potential biomarker and can be widely utilized in cancer diagnosis.

Citation: Kaneko K, Yamaguchi H, Saito T, Yano T, Oono Y, et al. (2014) Hypoxia Imaging Endoscopy Equipped with Laser Light ?Source from Preclinical Live Animal Study to
?First-In-Human Subject Research. PLoS ONE 9(6): e99055. doi:10.1371/journal.pone.0099055

Editor: Michael R Emmert-Buck, National Cancer Institute, National Institutes of Health, United States of America

Received March 24, 2014; **Accepted** April 17, 2014; **Published** June 10, 2014

Data Availability: The authors confirm that all data underlying the findings are fully available without restriction. All data are included within the manuscript.

Funding: *This work was supported in part by the National Cancer Center Research and Development Fund (23-A-45) and (23-A-15) and the 3rd-term* comprehensive 10-Year strategy for Cancer Control by the Ministry of Health, Labour and Welfare, and Accelerating Regulatory Science Initiative (H-24) [http://www.ncc.go.jp/en/index.html]. The funders had no role in study design, data collection and analysis, decision to publish, or preparation of the manuscript.

Competing Interests: *H. Yamaguchi and T. Saito are employees of FUJIFILM Corporation. This technology has been developed to apply to an endoscope* system. K. Kaneko has received grant support and a prototype endoscope system with hypoxia imaging function from Fujifilm Corporation, Tokyo, Japan. This does not alter our adherence to all the PLOS ONE policies on sharing data and materials.

* *E-mail: kkaneko@east.ncc.go.jp (KK); hiroshi.mm.yamaguchi@fujifilm.com (HY)*

Introduction

The cancer microenvironment is highly heterogeneous and hypoxia is strongly associated with the biological features of cancer [1]–[7]. Moreover, increasing evidence suggests that hypoxia is a critical component of cancer stem cell niche [8]. Thus, examinations into cancer hypoxia have been performed [9]–[11], but measurements having sufficient spatial-temporal resolution remain to be established.

Endoscopy is a suitable method for directly accessing the inside of the body and observing the cancerous lesion at high resolution. Therefore, an endoscope that can visualize the cancer microenvironment will open up new opportunities for cancer diagnosis and biological studies.

However, current methods, including fluorescent labelling techniques [12], [13] and hemoglobin absorption-based techniques [14]–[16], are limited in their applications to endoscope systems. In fluorescent labelling techniques, the spatial distribution of fluorescence is blurred because of a lack in specificity, low target accumulation, prolonged high retention and background, although improvements in agents continue to be made. In hemoglobin absorption-based techniques, many spectral images are required to detect the spectral differences between oxy- and deoxy-hemoglobin. Capturing variable wavelength images is time-consuming and the results are often blurred because the target does not remain in a state of rest under endoscopic observation.

Results

Development of hypoxia imaging technology

Herein, we developed an imaging technology that can derive the oxygen saturation (StO_2) images from small numbers of wavelength measurements. There were two challenges in deriving the StO_2 of the tissue in alimentary tracts from the differences in absorption spectra between oxy- and deoxy-hemoglobin using small numbers of wavelengths. First, the difference in optical absorption spectra in visible light region is small and the bandwidth between isosbestic points is very narrow. Second, reflectance of a tissue depends on hematocrit (Hct) as well as StO_2, because light absorption increases according to increases in hemoglobin density.

Selection of wavelength and bandwidth is vitally important in deriving StO_2 from small numbers of wavelength images. We found that a combination of narrow and two broad-band spectra are most suitable for derive StO_2 in alimentary tract tissue. (i) A narrow band at 473 nm was selected to detect the variations in StO_2, while the change in reflectance according to the variance in StO_2 at 473 nm is largest in the visible light region. We made the bandwidth very narrow (a few nanometres in width) to prevent a decrease in StO_2 sensitivity caused by wavelength width across the isosbestic points. (ii) A green broad-band was selected to detect variations in Hct. The green band is sensitive to variations in Hct because the absorption coefficient of hemoglobin is large. To make the signal robust to variations in StO_2, we broadened the green band (500–600 nm) across a few isosbestic points. (iii) A red broad-band was selected to detect the changes in illumination caused by the distance between the light exit window of the endoscope and the illuminated tissue. The red broad-band (600–700 nm) is robust to variations in StO_2 and Hct because the absorption coefficient of hemoglobin is small. We applied a computational technique to derive StO_2 signals from these three light signals. Briefly, the 473 nm signal and the green band signal are normalized against the red signal to cancel their dependence on illuminance. The normalized 473 nm signal is calibrated using the normalized green signal to cancel its dependence on Hct. Thus, pure StO_2 information can be obtained (Fig. 1A).

Based on these strategies, we developed an imaging system equipped with laser diodes of 445 and 473 nm and a white fluorescent pigment body. Broad-band diffused light is emitted from the white fluorescent pigment body excited by the 445-nm laser diode. The 473-nm diffused light, which is useful for illuminating narrow band light for StO_2 signals, is emitted by switching the laser light source from 445 nm to 473 nm. A color CCD sensor captures the 473-nm narrow band, and the green and red broad-band images (Fig. 1B).

In order to clarify the changes in quantity of light according to StO_2 and Hct, we introduced an intralipid phantom consisting of a

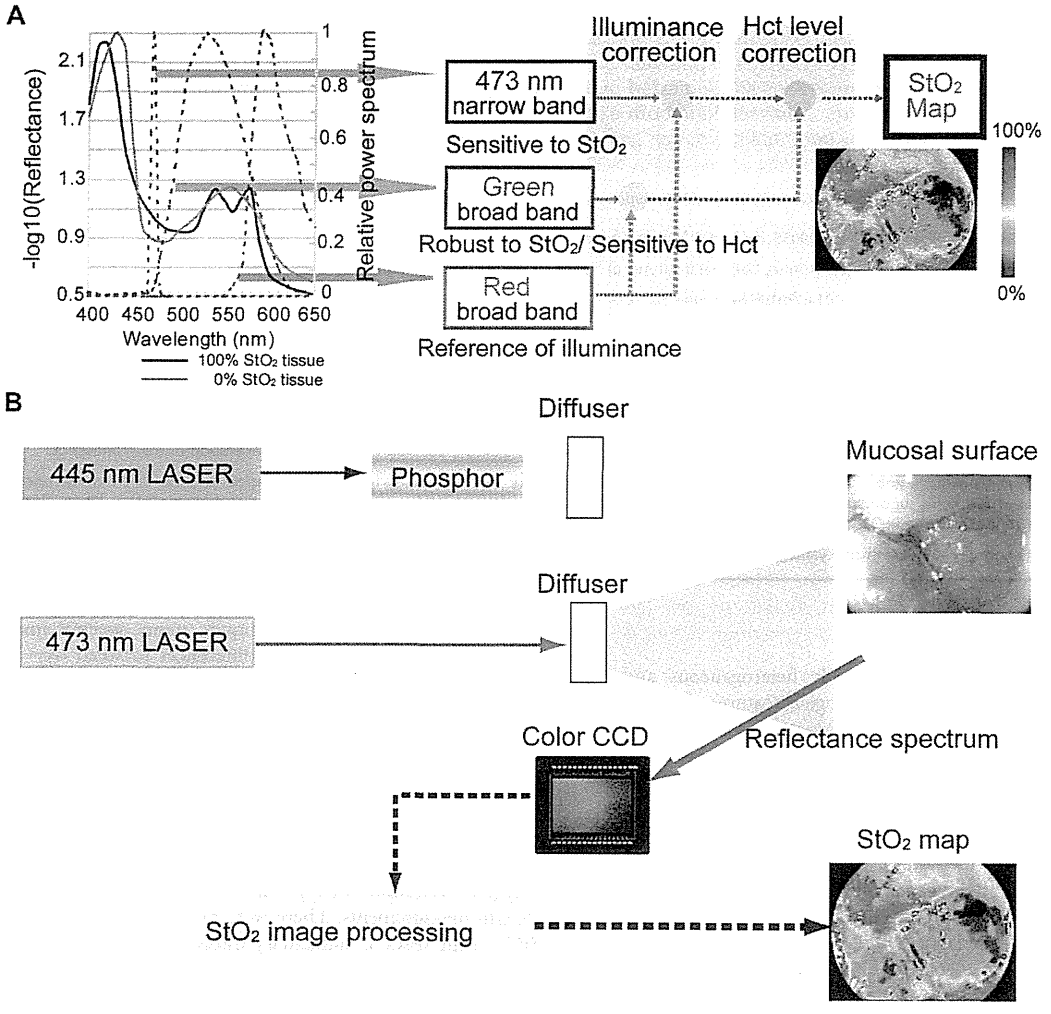

Figure 1. Mechanism of hemoglobin oxygen saturation imaging and schematic illustration of prototype endoscope system. (A) Illustration of the mechanism (see text for details.) (B) The 445-nm laser excited a phosphor equipped at the tip of the endoscope and emitted white light. The 473-nm laser light was emitted without the phosphor excitation. These two lights alternately illuminated the mucosal surface and the reflected lights were sequentially detected with a colour CCD in synchronization with light switching. The obtained images were processed and transformed into a StO_2 map.
doi:10.1371/journal.pone.0099055.g001

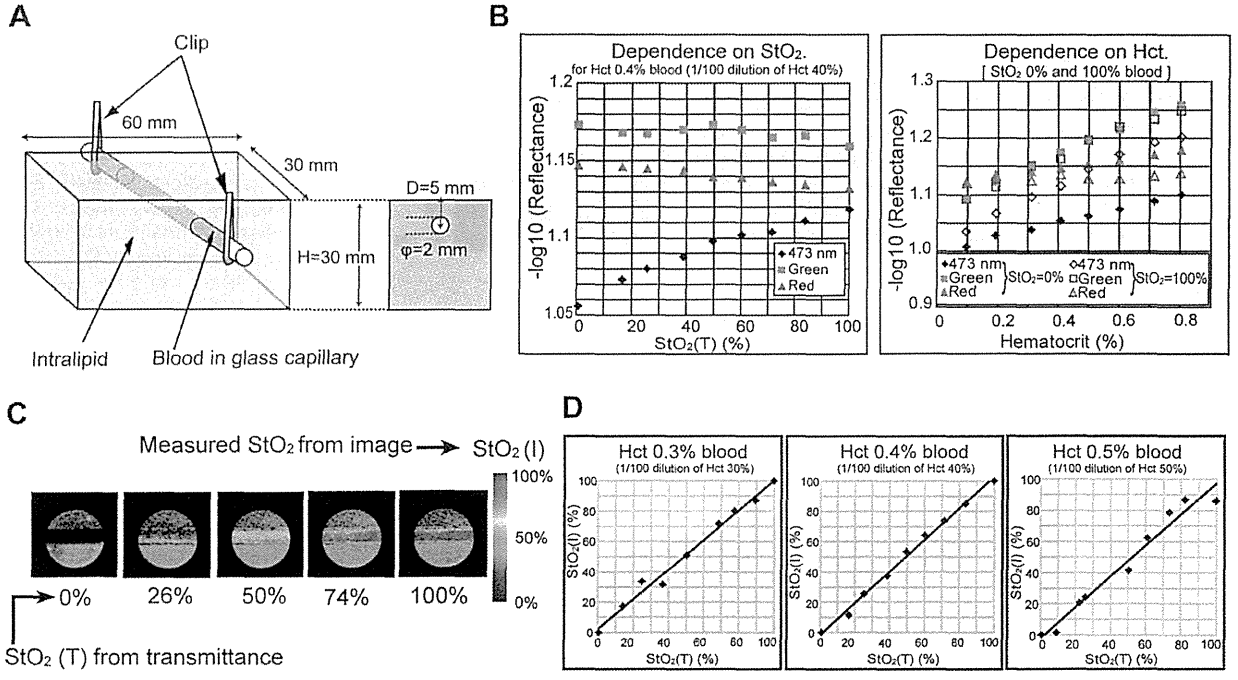

Figure 2. Verification of hemoglobin oxygen saturation imaging by observing a phantom. (A) Blood vessel phantom consisted of a glass tube filled with diluted blood and aqueous solution of intralipid. The intralipid solution strongly scattered incident light to simulate the living tissue around blood vessel. (B) The observed optical densities of the blood vessel at the three bands were dependent on StO2(T) (left) and Hct (right). Here, StO2(T) denotes the supposedly correct value of StO2 derived by analyzing the transmittance spectrum of blood. (C) StO2(I) map (derived by image processing) of the vessel. (D) Comparison of StO2(I) with StO2(T) (derived by measurement of transmittance spectra).
doi:10.1371/journal.pone.0099055.g002

glass capillary containing blood (Fig. 2A). The quantities of light as a function of StO_2 and Hct for 473 nm in the narrow, broad green and red bands were captured by the imaging system. Figure 2B shows that the 473 nm signal is sensitive to the change in StO2 and the green and red broadband signals are robust to that. Images were processed to create hemoglobin saturation maps. Figure 2C shows representative hemoglobin saturation pseudocolor maps of blood for different StO_2 levels. Measurements of hemoglobin saturation for different Hct levels derived with the imaging system corresponded well with the StO_2 measured using a spectral meter (Fig. 2D).

In vivo imaging of nude mouse transplanted with cancer cells

We then examined our approach using animal models. We used nude mice transplanted with A549 human cancer cells and attached window chambers [17] to the skin-peeled area, which kept the skin extended and enabled us to observe blood vessels under the skin. A549 cells were transplanted under the skin in the chambers (Fig. 3A). Three-band wavelength images using the imaging system to derive the StO_2 map from spectroscopic data were obtained (Fig. 3B left). The StO_2 map at 7 days after transplantation showed that the low StO_2 area was merged with the tumor-injected region where the tumor mass and aberrant tumor angiogenesis were augmented (Fig. 3B right). We confirmed the presence of cancer cells in histological images (Fig. 3C).

In vivo imaging of alimentary tracts with pigs

We then conducted an *in vivo* imaging experiment in pigs with a hypoxic area in the stomach tissue generated by transcatheter arterial embolization. Figure 4A shows a series of fluoroscopic images from the injection of the agent to embolization. Before embolization, high StO_2 value was observed (Fig. 4B lower left). Five minutes after embolization, the StO_2 map showed emergence of a hypoxic area corresponding to artificial vessel occlusion (Fig. 4B lower right). We also observed the change in StO2 at the esophagus. The StO2 was initially normal (around 70%) (Fig. 4C(i)). After the stomach removal, it declined to around 50–60% (Fig. 4C (ii)). The StO2 further dropped to near zero after the KCl injection (Fig. 4C (v)).

Human subject research

Next, we conducted a proof-of-the-concept research [18] for 40 patients with neoplastic lesions in the esophagus including the pharynx, stomach and colorectum (Table 1). In this first in human subject research (UMIN 000004983), two types of StO_2 images were used. One was a pseudocolor StO_2 image that showed StO_2 levels as different hues, and the other was a StO_2 overlay image that overlapped StO_2 levels in blue on a white light illumination image to detect background mucosa. Figure 5A shows an example of the StO_2 map for rectal adenocarcinoma. The hypoxic area was completely visible on the StO_2 map corresponding to the cancer region. Pathological diagnosis by H&E (hematoxylin and eosin) staining showed adenocarcinoma infiltrating into the submucosal layer (Fig. 5B upper). In this case, HIF1 alpha expression in immunohistochemical staining was found in the area described as hypoxic on the StO_2 map (Fig. 5B lower).

The hypoxic area was confirmed in early cancer. Eight colorectal adenomas with histological low-grade atypia were also detected as hypoxia, ranging between 3 mm and 10 mm in

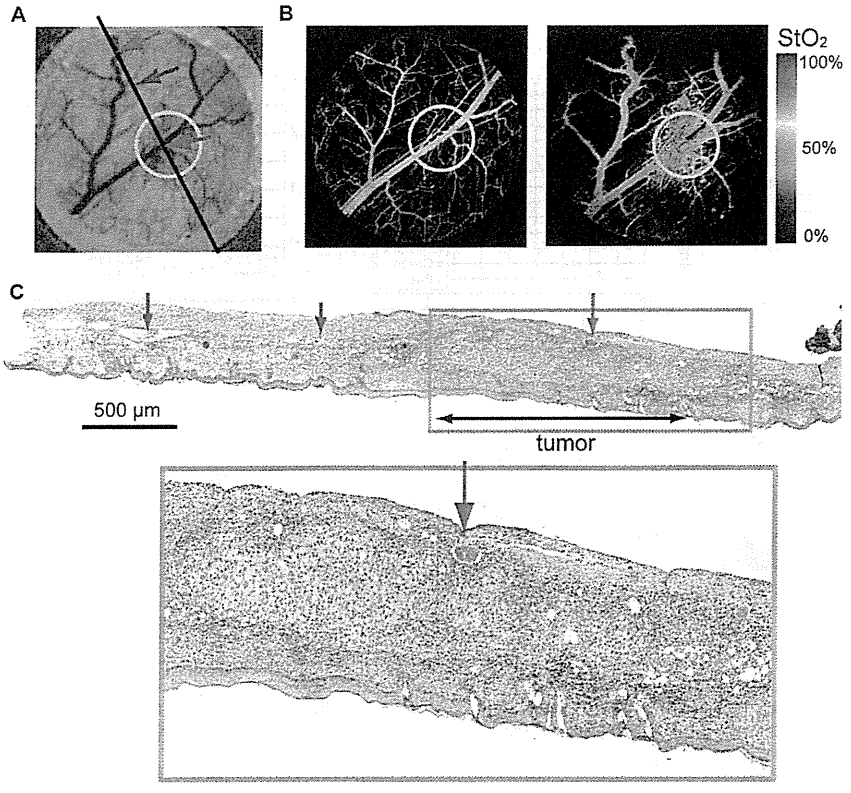

Figure 3. *In vivo* imaging of nude mouse implanted with cancer cells. (A) White light image of the mouse. The solid line corresponds to the cross-section of pathological assessment. (B) StO2 map of mouse before transplantation (left). Hypoxia developed at the tumor at 7 days after transplantation (right). (C) Histological picture (hematoxylin-eosin stained) of skin resected from the mouse at 14 days after transplantation (upper right, lower). Arrows indicate corresponding vessels.
doi:10.1371/journal.pone.0099055.g003

diameter (Fig. 5C upper, Video S1). Furthermore, one of the eight adenomas showed co-lesions combined with adenoma and hyperplasia. The low StO_2 region was detected in the adenoma portion, but not in the hyperplasic portion (Fig. 5C lower).

Figure 5D shows the observed StO_2 differences between neoplastic and non-neoplastic areas. Median StO_2 differences between neoplastic and non-neoplastic areas in the pharynx, esophagus, stomach and colorectum were −15.4%, −14.5%, −5.1% and −21.5%, respectively. There were significant differences in StO_2 levels between neoplastic and non-neoplastic areas in the esophagus ($p = 0.0078$ on Wilcoxon signed-rank test, 8 patients in each area ($n = 8$)) and colorectum ($p = 0.0001$, $n = 14$), but not in the stomach ($p = 0.9341$, $n = 15$) or pharynx ($p = 0.2500$, $n = 3$). Furthermore, sensitivity of neoplasia, defined as the proportion having correctly detected neoplasia, in the pharynx, esophagus, stomach, and colorectum was 67%, 100%, 33% and 86%, respectively.

Discussion

This is the first human subject research using the endoscopic hemoglobin oxygen saturation imaging technology for patients with aero-digestive tract cancers or adenomas. Before the human subject research, we evaluated our technology using a phantom and animals.

From the results of the phantom experiments, we confirmed that the green signal is useful for the separation of StO_2 and Hct information from the 473 signal. The characteristic that the red signal is robust to Hct and StO_2 is also important for the endoscopic application. The movement of the endoscope and alimentary tract tissue causes the change in illuminance during endoscopic observations. The robustness of red signal to Hct and StO_2 enables us to correct the change in illuminance.

Using dorsal skin-fold chamber mouse model, we detected temporal and spatial heterogeneity of oxygen saturation in tumor region. In a previous study [16], similar results were obtained using a hyperspectaral imaging system. The hyperspectral imaging system acquired images from 500 to 575 nm in 5-nm intervals to derive StO_2 map. We consider the hyperspectral imaging system needs long imaging times and a high-power source for sample illumination. Advantages of our technology in endoscopic application are short imaging times and the simplicity of the instruments. In *in-vivo* imaging experiments with pigs, we confirmed that our hypoxia imaging technology with endoscope can visualize the StO_2 map of alimentary tract tissue in real-time.

From the results of our human subject research, we can see that hypoxic imaging could clearly distinguish neoplasia from non-neoplasia in the esophagus and colorectum. As clinical benefits, screening of oesophageal and colorectal neoplasia, or prediction to efficacy of chemotherapy or radiotherapy can be utilized. Compared to the esophagus and colorectum, gastric cancer showed variations in tumor oxygen levels. Some cases exhibited hyperoxic conditions when compared with noncancerous areas around gastric cancer, but no significant differences were observed in

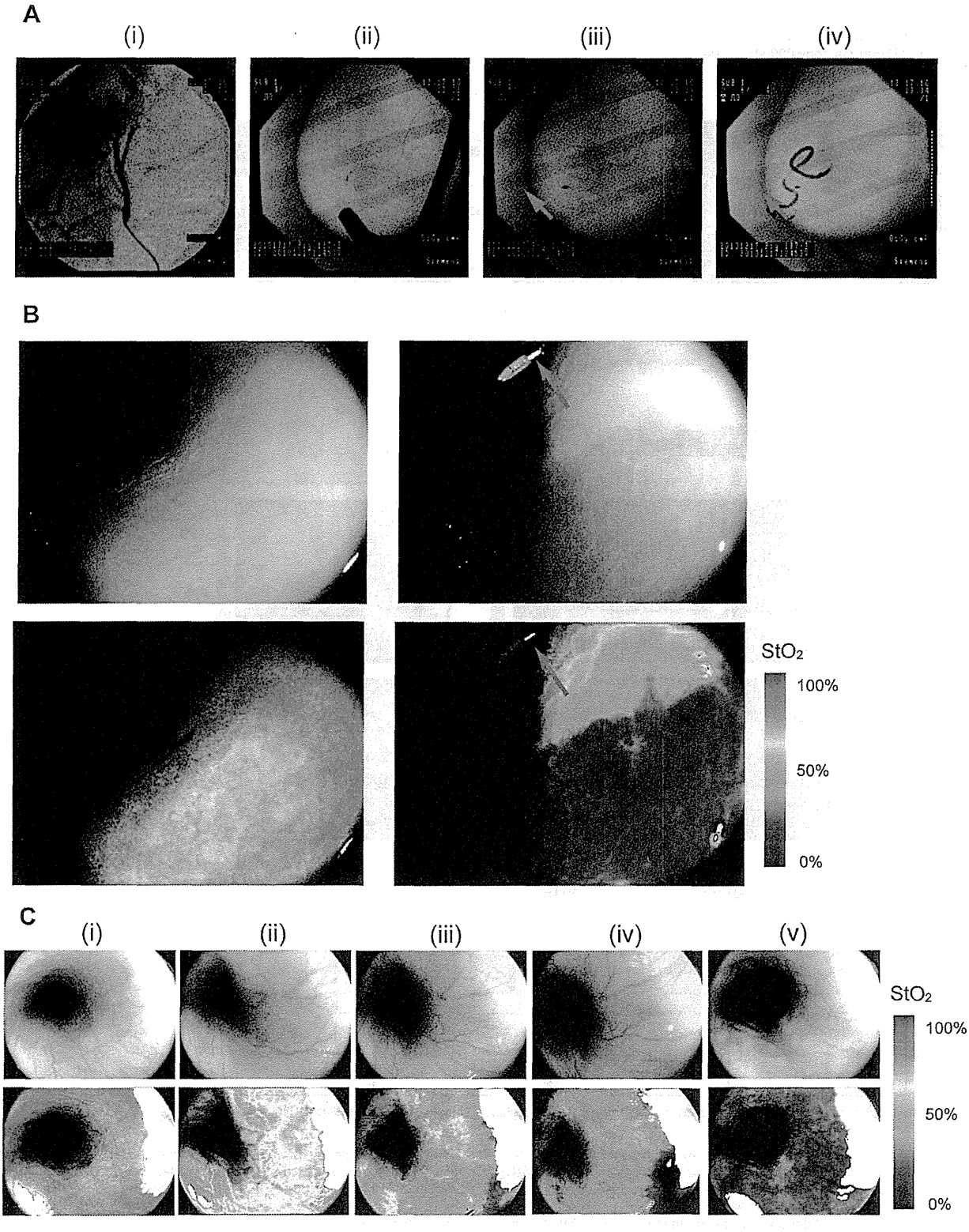

Figure 4. ***In vivo*** **imaging with pig.** (A) X-ray fluoroscopic images during application of transcatheter arterial embolization in pig stomach. (i) Image of the target vessel. (ii) Image of the endoscope inserted into the stomach. (iii) Red arrow indicates marking clip to identify the target area. (iv) Image of injected hystoacryl medium into the artery from the catheter. (B) White light images (upper) and StO_2 maps (lower) of the gastric mucosal surface visualized by laser endoscope system before embolisation (left) and five minutes after embolisation (right). (C) White light images (upper) and

StO_2 maps (lower) of the esophagus tissue (i) before the stomach removal, (ii) after the stomach removal, (iii) two minutes after the KCl injection, (iv) four minutes after the KCl injection and (v) twenty minutes after the KCl injection.
doi:10.1371/journal.pone.0099055.g004

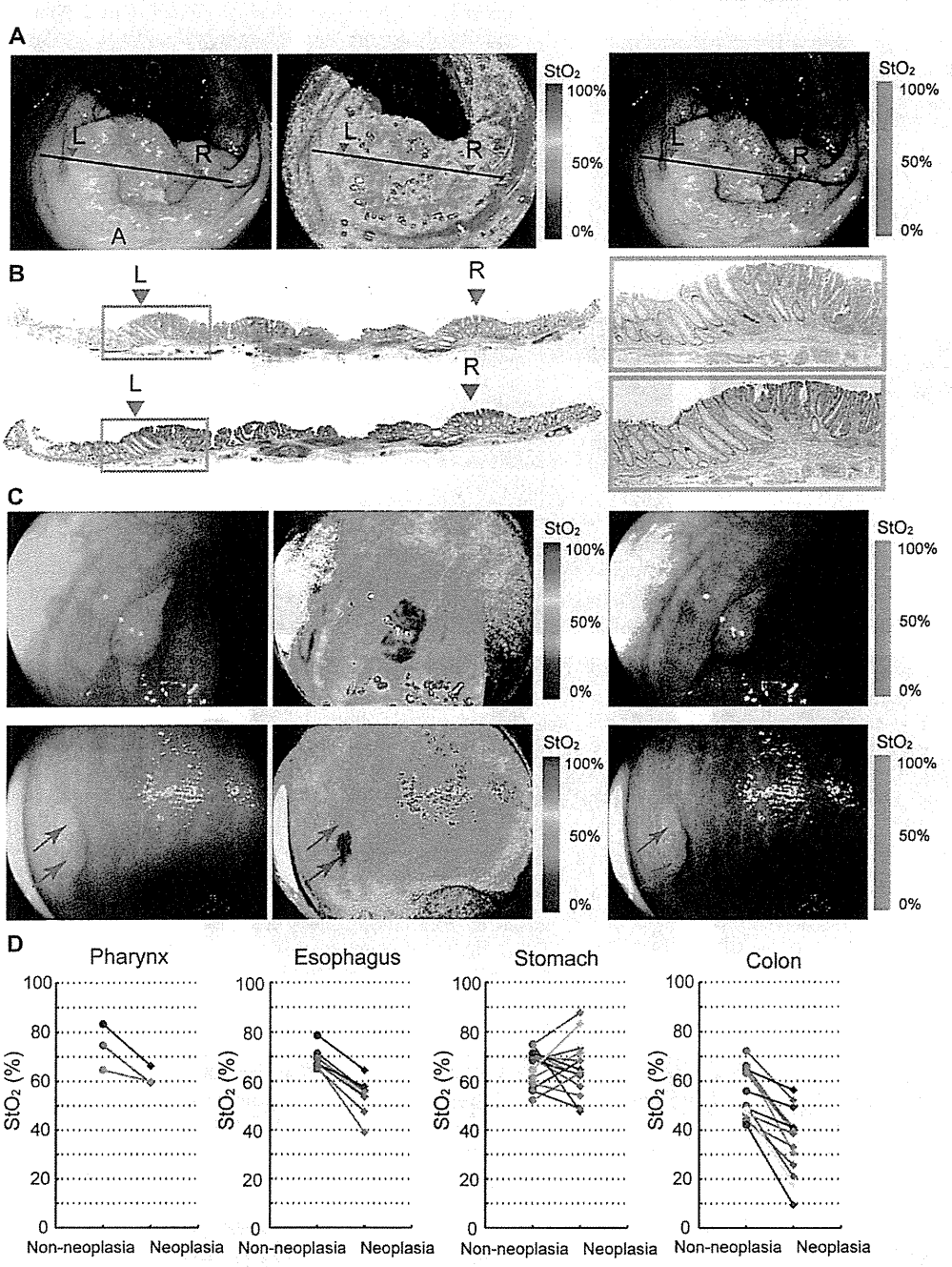

Figure 5. StO_2 maps obtained in human subject research. (A) White light image by endoscopic observation in rectal adenocarcinoma (left). Line (L-R) corresponds to cross-section of pathological diagnosis. StO_2 map visualized by laser endoscope system (middle: pseudocolor StO_2 image; right: StO_2 overlay image). (B) Cross-section appearance stained with H&E (upper) and HIF1 alpha antibody (lower) corresponding to the hypoxic area visualized with StO_2 map. (C) Endoscopic images of a colorectal adenoma (upper) showing clear hypoxia: white light image (upper left), pseudocolor StO_2 map (upper middle) and overlayed image (upper right). Another case of a colonic lesion (lower) consisting of an adenoma (red arrow) and a hyperplasia (blue arrow): white light image (lower left), pseudocolor StO_2 map (lower middle) and overlayed image (lower right). Only the adenoma was detected as hypoxia. (D) Observed StO_2 differences between neoplastic and non-neoplastic areas: For comparing pathology specimens and endoscope images, the line on the endoscopic image corresponding to the cross-section was determined. StO_2 levels at neoplasic and non-neoplasic areas along this line were then calculated using this StO_2 map.
doi:10.1371/journal.pone.0099055.g005

Table 1. Patients Characteristics.

(n = 40)	
Age	
Mean (y)	70.8
Range (y)	49–85
Gender n (%)	
Male	32 (80%)
Female	8 (20%)
Location n (%)	
Pharynx	3 (7%)
Esophagus	8 (20%)
Stomach	15 (38%)
Colorectum	14 (35%)

doi:10.1371/journal.pone.0099055.t001

clinicopathological findings between hypoxic cases and non-hypoxic including hyperoxic cases (Table 2). Further examination of organ specific hypoxia will be required.

Our endoscopic hypoxia imaging method provides a better opportunity to investigate the characteristics of cancer hypoxia. Some techniques detecting hypoxia by capillary methods, molecular biologic analysis and immunohistochemistry using histologic specimens have been reported. In the capillary method and molecular biological analysis [19], hypoxic conditions can be observed in only limited parts of the whole tumor, and features of whole tumors with hypoxia cannot be visualized. On immunohistochemistry using histologic specimens, visualization in real time is impossible. However, hypoxia imaging using this system is superior in visualizing the hypoxic conditions of whole tumors both sequentially and in real-time. No other method can simultaneously monitor oxygen concentrations in both cancerous and noncancerous areas.

Table 2. Clinicopathological findings of the study with gastric cancer patients.

		Hypoxia (n = 9)	Non-hypoxia (n = 6)
Age (y)	≥ 70 (n = 9)	5 (56%)	4 (44%)
	<70 (n = 6)	4 (67%)	2 (33%)
Gender	Male (n = 11)	6 (55%)	5 (45%)
	Female (n = 4)	3 (75%)	1 (25%)
Histologic type	Dif. (n = 12)	7 (58%)	5 (42%)
	Undif. (n = 3)	2 (67%)	1 (33%)
Macroscopic type	Elevated (n = 4)	3 (75%)	1 (25%)
	Depressed (n = 11)	6 (55%)	5 (45%)
Size (cm)	≥ 2 (n = 7)	5 (71%)	2 (29%)
	<2 (n = 8)	4 (50%)	4 (50%)
Location	U (n = 1)	1 (100%)	0 (0%)
	M (n = 10)	5 (50%)	5 (50%)
	L (n = 4)	3 (75%)	1 (25%)

doi:10.1371/journal.pone.0099055.t002

Our data strongly suggest that the microenvironment of oxygen supply to the tumor is spatially and temporally heterogeneous. This endoscope system enables us to observe spatial and temporal information of hypoxic conditions in human tumors. Moreover, we can directly acquire human cancer cells under various hypoxic conditions from biopsy samples. From these features, this endoscope system is expected to contribute to research into cancer biology, as well as into medications and treatment methods based on cancer hypoxia.

Methods

Ethics statement

This human subject research was approved by the National Cancer Center Hospital East Institutional Review Board (K23-2). A written informed consent was obtained from each patient. Animal experiments were approved by the Animal Ethics Committee of the National Cancer Center Hospital East (K13-015). We used horse blood, which was purchased from Nippon Bio-test Laboratories Inc., in the phantom experiment. The animal work that produced the blood samples was approved by the Animal Ethics Committee of the Nippon Bio-test Laboratories Inc.

Laser endoscope system

We developed a prototype laser endoscope system composed of two types of laser and a white fluorescent pigment body (20 mW, 473 nm laser diode, and 1 W, 445 nm blue laser diode; Nichia, Japan) as light sources and a commercial endoscope system (EG-590ZW gastroscope, and EC-590ZW3 colonoscope; Fujifilm, Japan).

Phantom

We created a vessel phantom composed of a glass microcapillary, Intralipid-10% (fat emulsion) and blood (horse blood, stored in an equal volume of Alsever's solution), inside a container of dimensions 60 mm×30 mm×30 mm (Fig. 2A). The vessel phantom imitates typical human tissue at a 100× magnified scale. The inside diameter of the glass microcapillary is 2 mm. The depth of glass microcapillary from the liquid surface is 5 mm. Thus, the vessel phantom imitates the 20-μm diameter vessel in human tissue at 50 μm depth. The size of the vessel is 100× magnified; therefore the scattering coefficient of Intralipid and absorption coefficient of blood is one hundredth that of typical human tissues. Blood is diluted with pure water so that the hematocrit value is 0.5%, 0.4% or 0.3%. Sodium hydrosulphite ($Na_2O_4S_2$) is used for de-oxygenation of blood. Transmittance spectra are measured with a spectral radiometer (TOPCON SR-UL1) and a Xenon light source, and the true value of oxygen saturation is calculated from transmittance spectra.

Dorsal skin-fold chamber mouse model

We anesthetized each mouse by intraperitoneal injection of 0.4 ml avertin (1.2 wt% 2,2,2-tribromoethanol and 1 wt% 2-propanol dissolved in saline). This treatment maintained the mouse under anethesia for about 30 min. To minimize pain, the following operation of mounting a window chamber was conducted within 15 min. We peeled a small part of the dorsal skin and then attached a custom-made skin-fold window chamber that kept the subcutaneous blood vessels in the skin-peeled area observable. The circular glass window was 9 mm in diameter. We prepared a suspension of A549 human lung cancer cells by mixing 2×10^5 cells with 40 μl of BD Matrigel™ and injected it under the

skin in the chamber. After the experiment, all the mice were sacrificed by deep euthanasia using diethyl ether.

Cell culture

A549 human lung cancer cells (ATCC) were cultured in Dulbecco's modified Eagle medium (DMEM) at 37°C.

In vivo imaging of alimentary tracts with pigs

We used two conventional female Large White and Duroc pigs (40 kg) bred in a closed colony. All efforts were made to minimize animal suffering. We anesthetized the pigs by firstly administration of 20 ml ketalar (500 mg/10 ml) intramuscularly and 250 mg isozol intravenously, and then inhalation of sevoflurane after intubation. Anesthesia was maintained via a circular breathing system. All the following procedures were carried out under the anesthesia. Under X-ray guidance with a fluoroscopic system (Powermobile C-ARM Angiographic System; Siemens), an angiographic catheter (Selecon safe tip; Terumo, Japan) was placed into the common hepatic artery, and a microcatheter (Progreat alpha; Terumo) was placed into the left gastroepiploic artery. We used Histacryl (B. Braun Biosurgicals) diluted 10-fold with Lipiodol (Terumo) as the embolic agent. We injected the agent with the micro catheter to embolize the arteries connected to the stomach. This embolization made the stomach partially hypoxic. The StO_2 map of the stomach was observed with the hemoglobin oxygen saturation imaging system. After the observation of the stomach, we opened the abdomen and removed the stomach for a histological evaluation. We also placed the endoscope at the esophagus and observed the change of the pig's oxygenation state before the stomach observation, after the stomach removal and after an intravenous administration of potassium chloride (KCl) to cause cardiac arrest.

Human subject research

Patients who had been confirmed to have pharyngeal, oesophageal, gastric, or colorectal neoplasia by previous endoscopic examination were enrolled. Eligibility criteria were as follows: age of 20 years or more; and male or female patients. After conventional endoscopy was performed, hypoxia imaging was observed using prototype endoscopy. To compare histologic findings to hypoxia imaging, all patients received endoscopic treatment, such as polypectomy, EMR or ESD after conventional and hypoxia imaging endoscopy. When comparing pathological findings, we determined the corresponding areas of neoplasia and non-neoplasia in the endoscope images and obtained StO_2 levels from the StO_2 map.

Pathological assessment

We performed immunohistochemical expression of HIF-1 alpha, which accumulates under hypoxia[5], to evaluate hypoxic status on the histological slide. Sections (5 μm) from paraffin-embedded slices that included the most representative area were selected and used for immunohistochemical staining of HIF-1 alpha (Rabbit polyclonal antibody to HIF-1 alpha(ab104072); Abcam, Tokyo, Japan). Citrate buffer (pH 6.0) was used for antigen retrieval, and antigen dilution was ×100. Human lung adenocarcinoma and squamous cell carcinoma were used as positive controls.

Statistical analysis

StO_2 levels were measured in both neoplastic and non-neoplastic areas for each patient. Stratified by cancer region, this paired data was compared using Wilcoxon signed-rank test. Among gastric cancer patients, we summarised the patient characteristics according to the remainder calculated by subtracting StO_2 levels of the normal tissue from those of tumor tissue, as in some cases, tumor tissue appeared as non-blue color (same color as normal tissues). All P values were two-sided.

Supporting Information

Video S1 Endoscopic video image showing the hypoxic feature of a colorectal adenoma in real time: white light image (left upper), pseudocolor StO_2 map (left lower) and overlayed image (right).
(ZIP)

Acknowledgments

We acknowledge the contributions of S. Tominaga (phantom experiment), T. Kobayashi, M. Satake, T. Kimura, M. Kobayashi, C. Yamauchi and Y. Shiraishi (*in vivo* imaging experiment), and H. Hasegawa (human subject research).

Author Contributions

Conceived and designed the experiments: KK HY AS HE AO. Performed the experiments: KK HY TS TY YO HI MK. Analyzed the data: HY TS SN. Contributed reagents/materials/analysis tools: TS SN. Contributed to the writing of the manuscript: KK HY.

References

1. Bertout JA, Patel SA, Simon MC (2008) The impact of O2 availability on human cancer. Nature Rev. Cancer 8: 967–975.
2. Hockel M, Schlenger K, Aral B, Mitze M, Schaffer U, et al. (1996) Association between tumour hypoxia and malignant progression in advanced cancer of the uterine cervix. Cancer Res. 56: 4509–4515.
3. Hanahan D, Weinberg RA (2011) Hallmarks of cancer: the next generation. Cell 144: 646–674.
4. Semenza GL (2003) Targeting HIF-1 for cancer therapy. Nature Rev. Cancer 3: 721–732.
5. Semenza GL (2008) Hypoxia-inducible factor 1 and cancer pathogenesis. IUBMB Life 60: 591–597.
6. Pennacchietti S, Michieli P, Galluzzo M, Mazzone M, Giordano S, et al. (2003) Hypoxia promotes invasive growth by transcriptional activation of the met protooncogene. Cancer Cell. 3: 347–361.
7. Sutherland RM (1998) Tumour hypoxia and gene expression—implications for malignant progression and therapy. Acta Oncol. 37: 567–574.
8. Keith B, Simon MC (2007) Hypoxia-inducible factors, stem cells, and cancer. Cell 129: 465–472.
9. Jordan BF, Runquist M, Raghunand N, Baker A, Williams R, et al. (2005) Dynamic contrast-enhanced and diffusion MRI show rapid and dramatic changes in tumour microenvironment in response to inhibition of HIF-1 alpha using PX-478. Neoplasia 5: 475–485.
10. Goh V, Engledow A, Rodriguez-Justo M, Shastry M, Peck J, et al. (2012) The flow-metabolic phenotype of primary colorectal cancer: assessment by integrated 18F-FDG PET/perfusion CT with histopathologic correlation. J. Nucl. Med. 53(5): 687–692.
11. Chitneni SK, Palmer GM, Zalutsky MR, Dewhirst MW (2011) Molecular Imaging of Hypoxia, J. Nucl. Med. 52: 165–168.
12. Zhang G, Palmer GM, Dewhirst MW, Fraser CL (2009) A dual-emissive-materials design concept enables tumour hypoxia imaging. Nature Materials 8: 747–751.
13. Harada H, Kizaka-Kondoh S, Hiraoka M (2005) Optical imaging of tumour hypoxia and evaluation of efficacy of a hypoxia-targeting drug in living animals. Mol. Imaging 4: 182–193.
14. Benaron DA, Parachikov IH, Friedland S, Soetikno R, Brock-Utne J, et al. (2004) Continuous, noninvasive, and localized microvascular tissue oximetry using visible light spectroscopy. Anesthesiology 100: 1469–1475.
15. Maxim PG, Carson JJ, Benaron DA, Loo BW Jr, Xing L, et al. (2005) Optical detection of tumours in vivo by visible light tissue oximetry. Technol. Cancer Res. Treat. 4: 227–234.
16. Sorg BS, Moeller BJ, Donovan O, Cao Y, Dewhirst MW (2005) Hyperspectral imaging of hemoglobin saturation in tumour microvasculature and tumour hypoxia development. J. Biomed. Opt. 10: 4400–4404.

17. Moy AJ, White SM, Indrawan ES, Lotfi J, Nudelman MJ, et al. (2011) Wide-field functional imaging of blood flow and hemoglobin oxygen saturation in the rodent dorsal window chamber. Microvasc Res. 82(3): 199–209.
18. Barkun JS, Aronson JK, Feldman LS, Maddern GJ, Strasberg SM, et al. (2009) Evaluation and stages of surgical innovations. Lancet 374: 1089–1096.
19. Brown JM, Wilson WR (2004) Exploiting tumour hypoxia in cancer treatment. Nature Rev. Cancer 4: 437–447.

ORIGINAL CONTRIBUTION

Clinical Impact of Elastic Laminal Invasion in Colon Cancer: Elastic Laminal Invasion-Positive Stage II Colon Cancer Is a High-Risk Equivalent to Stage III

Mitsuru Yokota, M.D.[1] • Motohiro Kojima, M.D.[2] • Shogo Nomura, M.Sc.[3]
Yusuke Nishizawa, M.D.[1] • Akihiro Kobayashi, M.D.[1] • Masaaki Ito, M.D.[1]
Atsushi Ochiai, M.D.[2] • Norio Saito, M.D.[1]

1 Division of Colorectal Surgery, National Cancer Center Hospital East, Kashiwa, Chiba, Japan
2 Division of Pathology, Research Center for Innovative Oncology, National Cancer Center Hospital East, Kashiwa, Chiba, Japan
3 Clinical Trial Section, Research Center for Innovative Oncology, National Cancer Center Hospital East, Kashiwa, Chiba, Japan

BACKGROUND: Elastic laminal invasion is defined as tumor invasion beyond the peritoneal elastic lamina. It is one of the factors affecting the prognosis of patients with colon cancer.

OBJECTIVE: This study aimed to investigate the clinical impact of elastic laminal invasion in colon cancer and the magnitude of the worse prognosis of elastic laminal invasion-positive, node-negative patients.

DESIGN: This was a retrospective cohort study.

SETTINGS: This study reviewed data from a tertiary care cancer center in Japan.

PATIENTS: The records of 436 patients with pT3 or pT4a colon cancer who underwent curative resection between January 1996 and December 2006 were reviewed.

MAIN OUTCOME MEASURES: The primary outcome measure was recurrence-free survival. Cox regression analyses established the factors associated with recurrence-free survival. Six groups formed by combining the factors were compared.

RESULTS: Of the patients with pT3 disease, those who were positive for elastic laminal invasion had a 5-year recurrence-free survival rate of 73.8% compared with a rate of 85.0% in those who were negative for elastic laminal invasion and 53.5% in patients with pT4 disease. Three unfavorable prognostic factors were identified, including lymph node metastasis, positive elastic laminal invasion, and a lack of adjuvant chemotherapy. Log-rank analysis revealed statistically significant differences in recurrence-free survival between group 1 (node negative, elastic laminal invasion negative, and no adjuvant chemotherapy) and group 3 (node negative, elastic laminal invasion positive, and no adjuvant chemotherapy). The HR for group 1 compared with group 3 was 0.49 (95% CI, 0.27–0.90). Furthermore, the HRs for group 2 (node positive, elastic laminal invasion negative, and received adjuvant chemotherapy) and group 4 (node positive, elastic laminal invasion positive, and received adjuvant chemotherapy) vs group 3 were 0.77 (95% CI, 0.35–1.69) and 1.36 (95% CI, 0.62–2.98).

LIMITATIONS: Our study has limited prediction accuracy of our prognostic stratification, and an analysis of small subgroups may not have been capable of detecting significant differences. In addition, a wide range of hematoxylin and eosin- and elastica-stained slides were examined per case.

CONCLUSIONS: Elastic laminal invasion adversely influences prognosis in pT3 and pT4a colon cancer. Although elastic laminal invasion positivity does not affect prognosis in node-positive patients receiving adjuvant chemotherapy, node-negative patients with elastic laminal invasion have a similar risk of recurrence as node-positive patients.

Funding/Support: Grant support for this study was provided by a National Cancer Center Research and Development Fund (23-A-14).

Financial Disclosure: None reported.

Presented at the Digestive Disease Week conference, Orlando, FL, May 18 to 21, 2013.

Correspondence: Norio Saito, M.D., Division of Colorectal Surgery, National Cancer Center Hospital East, 6-5-1 Kashiwanoha, Kashiwa, Chiba 277–8577, Japan. E-mail: norsaito@east.ncc.go.jp

Dis Colon Rectum 2014; 57: 830–838
DOI: 10.1097/DCR.0000000000000124

KEY WORDS: Colon cancer; Elastic laminal invasion; High-risk stage II; Serosal invasion.

In 2008, 1.2 million people received a new diagnosis of colorectal carcinoma (CRC), and 608,700 patients died of the disease, making it the fourth most common cause of cancer death globally.[1] However, in the United States and Europe, it is the second leading cause of cancer death.[2,3] In Japan, CRC is diagnosed in ≈105,000 patients each year and accounts for 42,000 deaths, making it the third leading cause of death from cancer.[4]

CRC is staged using the TNM system of the International Union Against Cancer (UICC),[5] in which primary tumor extension (T), regional lymph node involvement (N), and the presence of distant metastasis (M) are established to guide treatment and predict prognosis. Pathologic (p) T categories are divided into pT1 to pT4: pT3 disease is defined by subserosal tumor invasion and accounts for approximately half of all cases of CRC. The prognosis of patients with pT3 disease varies, which may be explained by differences in the depth of tumor invasion.[6–8] Nevertheless, although it has been suggested that pT3 disease be subclassified, it currently remains 1 category.

The peritoneal elastic lamina (PEL) is a component of the normal intestinal wall and can be identified histologically by elastica staining. It is situated beneath the visceral peritoneum and covers the intestinal wall. Subclassifying pT3 tumors according to their relationship with the PEL has been suggested as another method of pT3 classification. Patients with tumor invasion beyond the PEL are classified as having elastic laminal invasion (ELI).[9] Furthermore, the elastic lamina is used as a landmark of invasion of the visceral pleura in the TNM classification of lung cancer.[5] These facts guide us to focus on the PEL as a landmark of the classification of tumor spread.

Our previous study of 564 patients with stage II to IV CRC suggested that ELI was one of the factors affecting the prognosis of patients with colon cancer (CC) and an independent risk factor for tumor recurrence only among CC patients with stage II disease.[10] However, it is not yet clear that ELI status can be a prognostic factor under comprehensive analysis, including factors such as lymph node involvement and adjuvant chemotherapy.

The aim of this study was to investigate the clinical impact of ELI in patients diagnosed with pT3 and pT4a CC and the magnitude of the worse prognosis of patients with ELI-positive, node-negative CC (NNCC).

MATERIALS AND METHODS

Patients Selection and Follow-up

Of the 1103 consecutive patients who underwent surgery for CC at the National Cancer Center Hospital East between January 1996 and December 2006, 721 patients had pT3 or pT4a disease. The following patients were excluded: 1) patients with multiple or metachronous CC, 2) patients simultaneously or previously diagnosed with an advanced tumor other than CC, 3) patients with distant metastasis, 4) patients who received neoadjuvant therapy, and 5) patients in whom resection was incomplete (R1 and R2). Completeness of resection was classified as R0 (negative gross and pathologic margins), R1 (negative gross and positive microscopic margins), and R2 (positive gross margins). R1 and R2 were defined as incomplete resection. After exclusions, the clinical records of 439 patients with pT3 and pT4a CC were retrospectively studied. We began routinely administering 5-fluorouracil–containing adjuvant chemotherapy for patients with stage III disease in 2003, and 3 patients with stage II CC were excluded because they had also received adjuvant chemotherapy. Each patient's prospectively collected demographic, staging, histopathology, and prognostic outcome data were recorded. All of the cases were reclassified based on the 7th edition of the UICC TNM staging system.[5] We did not categorize isolated tumor deposits as pN1c to avoid overestimating the prognosis of patients with stage III disease. Follow-up after surgery was composed of serum tumor marker measurement every 3 months and chest and abdominal CT every 6 months for the first 3 years, then every 6 months for the next 2 years, and annually for 2 additional years. All of the patients were followed from the date of surgery to the last contact (death or last follow-up) or until December 31, 2011. Recurrence was defined as distant metastasis, local recurrence, or peritoneal dissemination; the final diagnosis was made by imaging (CT, MRI, and/or positron emission tomography CT), cytologic analysis, or biopsy, if necessary.

Written, informed consent to tissue collection and use for research was obtained. Conduct of the study was approved by our local ethics committee (National Cancer Center Hospital, No. 2012-067).

Histopathologic Analysis

We used the same histopathologic protocol as our previous study.[10] The resected specimens were fixed in 10% formalin, and the entire tumor was cut into 5-mm sections. Representative slices were embedded in paraffin, cut into 3-μm sections, and stained with hematoxylin and eosin (H&E) and elastica stain to allow evaluation of serial sections for ELI status and lymphovascular invasion (Fig. 1). We used the modified resorcin-fuchsin method for the latter.[11] There is a defect of the PEL at the mesenteric attachment; therefore, we undertook elastica staining on at least 1 whole section where the tumor was closest to the peritoneal surface to confirm the continuity of the PEL. The median numbers of H&E- and elastica-stained sections were 6 (range, 2–20) and 4 (range, 2–16). We defined cases with tumor invasion beyond the PEL as ELI positive (Fig. 1C

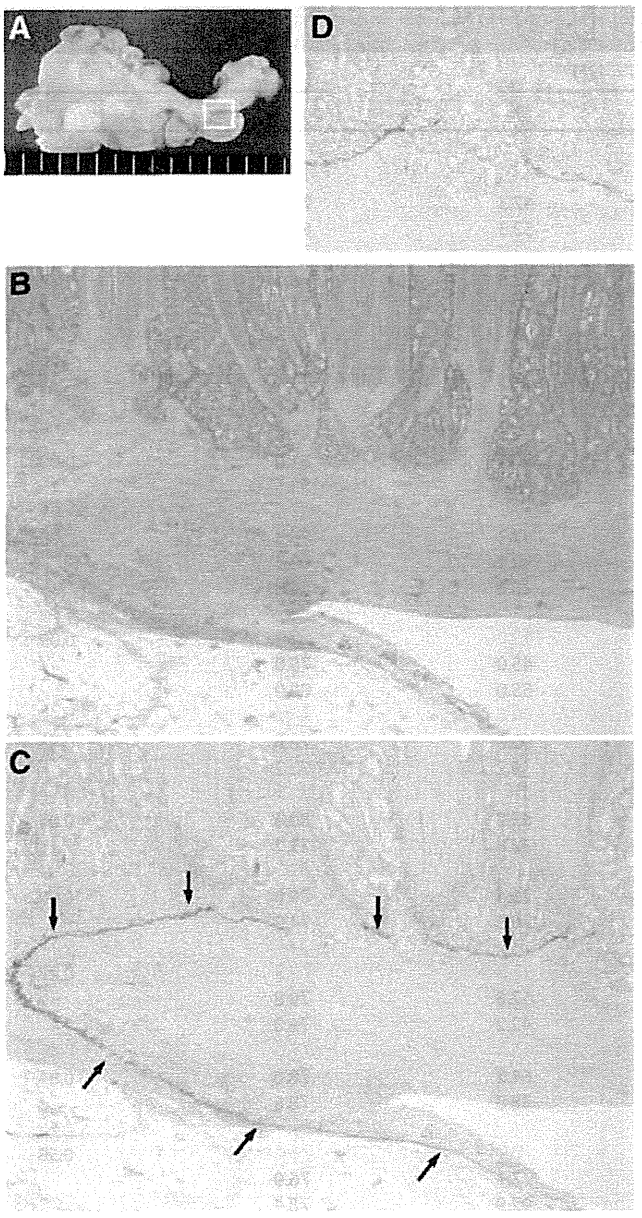

FIGURE 1. A, Cut surface of a tumor with elastic lamina invasion (ELI). Hematoxylin and eosin staining (B; ×40) and elastica staining (C; ×40; D, ×100) of the white box area in A. The peritoneal elastic lamina (PEL; arrows in C) is situated beneath the visceral peritoneum. C and D, Tumor invasion beyond the PEL represents ELI positivity.

and 1D). Continuity of the PEL in unaffected areas was confirmed regardless of the intensity of staining near the tumor. In cases with duplication of the PEL around the invasive front of the tumor, we determined cases with tumor invasion beyond the PEL to be ELI positive only when the PEL was judged the outermost layer of elastin. In cases in which the PEL had been disrupted, its estimated course was obtained by drawing a straight line between the residual PEL; only cases with invasion beyond the line were defined as ELI positive. ELI status was retrospectively evaluated by 2 pathologists blinded to the patient outcomes.

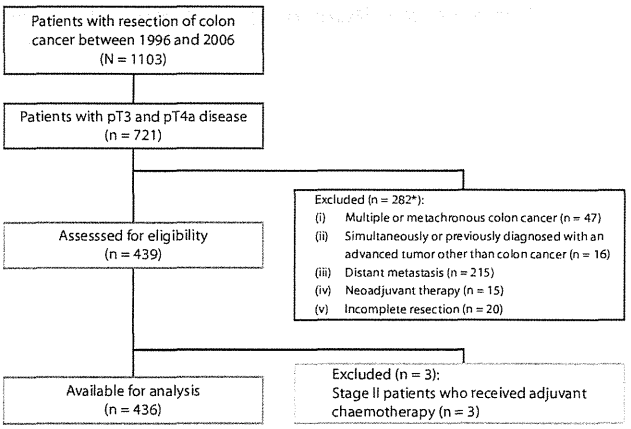

FIGURE 2. Consolidated Standards of Reporting Trials diagram of the study. *At least 1 of the criteria (i to v) was met.

Statistical Analysis

Our primary outcome measure was recurrence-free survival (RFS), defined as the time that elapsed between the date of surgery and any relapse or death from any cause. Overall survival (OS) was a secondary outcome, defined as the time from surgery to death from any cause. We chose RFS as the primary outcome to avoid the impact of treatments after recurrence on survival. Kaplan-Meier survival curves were plotted and compared using the log-rank test. Continuous variables were separated into 2 categories on the basis of their median values. All of the baseline characteristics were summarized as numbers and percentages.

To verify whether ELI status was an independent prognostic factor, we first performed multivariate Cox regression analyses for RFS. Baseline covariates included age (<65 or ≥65 years), sex (male or female), tumor size (<4.5 or ≥4.5 cm), histologic differentiation (well/moderately or poorly/mucinous), surgical technique (open or laparoscopic), lymphatic invasion (positive or negative), venous invasion (positive or negative), lymph node metastasis (positive or negative), number of lymph nodes retrieved (less than 12 or 12 or more), preoperative serum CEA level (<5 or ≥5 ng/mL), adjuvant chemotherapy (received or not received), and ELI (positive or negative).

The branch-and-bound algorithm of the Furnival and Wilson[12] variable selection procedure was applied to identify the risk factors using these candidate covariates. Next, we divided patients into all of the possible combinations based on the covariates identified in the Cox regression analyses so that their stratification would be meaningful. To establish the extent to which ELI adversely affected prognosis in NNCC, we compared the group consisting of patients with ELI-positive NNCC with groups composed of patients with node-positive CC (NPCC; stage III disease). We also applied the risk group to patients with pT3, because exclusion of patients with pT4a disease might have influenced our proposed risk stratification. Furthermore, we evaluated how the risk group affected OS.

TABLE 1. Patient characteristics and univariate analysis for RFS

	No. of patients (N = 436)		RFS	
Variable	*No.*	*%*	*5 y (%)*	*p[a]*
Age, y				
Median (range)	65.0 (26.0–92.0)			0.32
<65	208	47.7	76.2	
≥65	228	52.3	80.5	
Sex				
Male	251	57.6	76.1	0.17
Female	185	42.4	81.1	
Tumor location				
Right	146	33.5	83.7	0.08
Transverse	51	11.7	71.4	
Left	239	54.8	76.3	
Tumor stage				
pT3	393	90.1	81.0	<0.0001
pT4a	43	9.9	53.5	
Nodal status				
pN0	250	57.3	88.3	<0.0001
pN1	140	32.1	68.4	
pN2	46	10.6	54.8	
Tumor size, cm				
Median (range)	4.5 (0.6–16.5)			0.09
<4.5	196	45.0	75.0	
≥4.5	240	55.0	80.9	
Histologic differentiation				
Well/moderately	396	90.8	78.8	0.38
Poorly/mucinous	40	9.2	72.2	
Lymphatic invasion				
Negative	293	67.2	80.6	0.07
Positive	143	32.8	73.2	
Venous invasion				
Negative	102	23.4	89.0	0.002
Positive	334	76.6	74.9	
CEA, ng/mL				
Median (range)	3.9 (0.2–247.7)			0.27
<5	252	57.8	79.8	
≥5	184	42.2	76.0	
Type of surgery				
Open	267	61.2	78.0	0.84
Laparoscopic	169	38.8	78.6	
No. of lymph nodes retrieved				
Median (range)	26.5 (4.0–124.0)			0.58
<12	31	7.1	76.0	
≥12	405	92.9	78.4	
Adjuvant chemotherapy				
Received	71	16.3	78.4	0.98
Not received	365	83.7	77.2	
ELI				
Negative	254	58.3	85.1	<0.0001
Positive	182	41.7	68.8	

ELI = elastic laminal invasion; RFS = recurrence-free survival.
[a]*p* value was calculated by log-rank test (2 sided).

All of the statistical analyses were performed using SAS 9.3 (SAS Institute, Cary, NC). All *p* values were reported as 2 sided, and statistical significance was defined as values <0.05.

RESULTS

Patient Characteristics

A total of 436 patients with a median age of 65.0 years were enrolled (Fig. 2). Their characteristics were shown in Table 1. Tumors were located in the cecum in 26 patients (6.0%), the ascending colon in 120 (27.5%), the transverse colon in 51 (11.7%), the descending colon in 36 (8.3%), and the sigmoid colon in 203 (46.5%). Tumors were classified as stage IIA, IIB, IIIB, and IIIC in 236 (54.1%), 14 (3.2%), 165 (37.9%), and 21 patients (4.8%). Seventy-one patients (38.2%) with stage III CC received adjuvant chemotherapy after primary resection. Overall, 182 patients

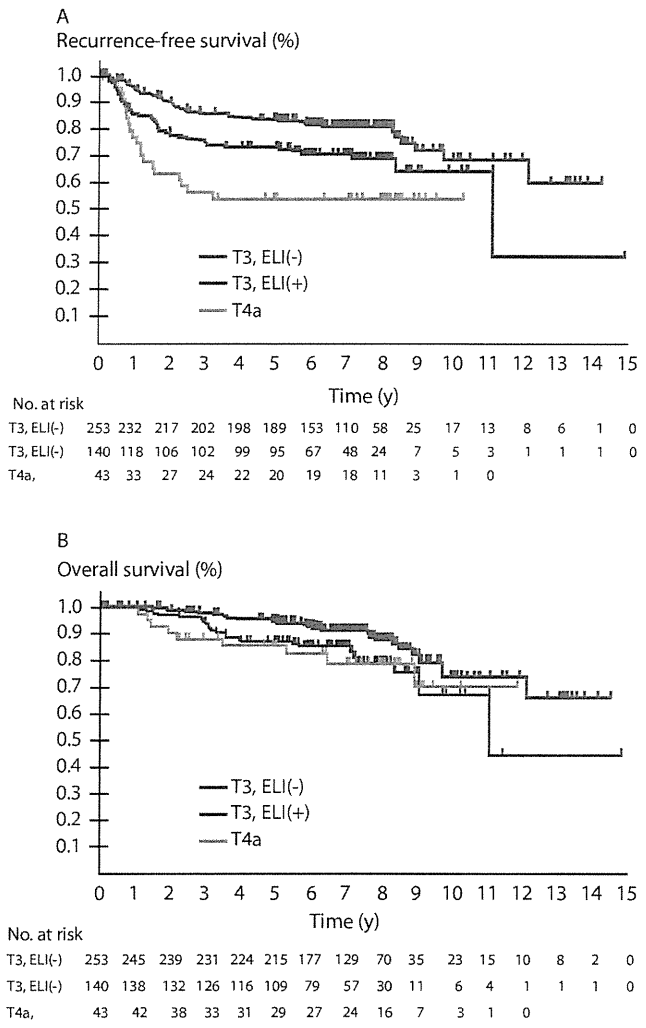

FIGURE 3. Kaplan-Meier curves depicting recurrence-free (A) and overall survival (B) based on the elastic laminal invasion status of 436 patients who underwent primary resection for colon cancer.

(41.7%) were identified as ELI positive, 140 (35.6%) of those with pT3 and 42 (97.7%) of those with pT4a disease.

Association Between ELI Status and Survival

The 5-year RFS and OS for all of the participants were 78.2% and 92.9%. The median follow-up was 7.1 years (range, 0.1–15.1 years). Of those who survived, 93.3% were followed for ≥3 years, and 88.0% were followed for ≥5 years. Tumor stage, nodal status, venous invasion, and ELI status influenced RFS (Table 1). Of the patients with pT3 disease, those who were ELI positive had a 5-year RFS of 73.8% compared with 85.0% for those who were ELI negative ($p = 0.002$) and 53.5% for patients with pT4 disease ($p = 0.02$; Fig. 3A). Tumors recurred in 95 (21.8%) of the 436 patients; the most common sites of recurrence were the liver (48 patients), lung (18 patients), and peritoneum (13 patients). The 5-year OS of ELI-positive patients with pT3 disease was 87.3% compared with 94.9% if ELI status was negative ($p = 0.02$) and 85.3% in patients with pT4 disease ($p = 0.82$; Fig. 3B). Overall, 63 patients died (14.4%): of those who died of CC, 28 were ELI positive and 14 were ELI negative; of those who died of other causes, 6 were ELI positive and 15 were ELI negative.

TABLE 2. Multivariate Cox regression analyses for RFS to assess the influence of risk factors

	RFS		
Variable	*HR*	*p*	*95% CI*
Lymph node metastasis (+)	2.96	<0.0001	1.95–4.49
Adjuvant chemotherapy (+)	0.50	0.01	0.29–0.85
ELI (+)	1.59	0.02	1.08–2.33

ELI = elastic laminal invasion; RFS = recurrence-free survival.

Multivariate Analyses

We performed Cox regression analyses on all 436 patients. For RFS, the branch-and-bound algorithm identified 3 unfavorable factors, including lymph node metastasis ($p < 0.0001$), lack of adjuvant chemotherapy ($p = 0.01$), and ELI positive status ($p = 0.02$; Table 2). Patients were divided into 6 groups based on these unfavorable factors, as shown in Table 3. We chose group 3 (node negative, ELI positive, and no adjuvant chemotherapy) as the reference value to compare with node-positive patients.

Evaluation of Prognosis

Kaplan-Meier curves for RFS in each group are shown in Figure 4A. The survival curves of group 5 (node positive, ELI negative, and no adjuvant chemotherapy) and group 6 (node positive, ELI positive, and no adjuvant chemotherapy) were almost identical ($p = 0.43$), and there was not a significant difference between group 2 (node positive, ELI negative, and received adjuvant chemotherapy) and group 4 (node positive, ELI positive, and received adjuvant chemotherapy; $p = 0.15$). There was, however, a significant difference between group 1 (node negative, ELI negative, and no adjuvant chemotherapy) and group 3 ($p = 0.001$). The RFS curve of group 3 lay between those of group 2 and group 4, both of which were composed of node-positive patients. The HR for group 1 vs group 3 was 0.49 (95% CI, 0.27–0.90), corresponding with a 51% relative reduction in the risk of recurrence. Furthermore, the HRs for groups 2 and 4 vs group 3 were 0.77 (95% CI, 0.35–1.69) and 1.36 (95% CI, 0.62–2.98).

When group 3 was compared with the other groups in terms of OS, similar trends were observed (Table 3 and Fig. 4B). The estimated OS Kaplan-Meier curve of group 3 was also between those of groups 2 and 4. The HRs for groups 2 and 4 vs group 3 were 0.88 (95% CI, 0.29–2.62) and 1.81 (95% CI, 0.61–5.41).

Findings After Exclusion of Patients With pT4a Disease

The impact of ELI status was reanalyzed using the same 6 groups after patients with pT4a disease were excluded

TABLE 3. Comparison of 5-year RFS and OS of the 6 stratified groups

Group		n	RFS		OS	
			5-y % (95% CI)	HR (95% CI)	5-y % (95% CI)	HR (95% CI)
1	N0,ELI(−),AC(−)	166	91.1 (85.4–94.6)	0.49 (0.27–0.90)	98.1 (94.2–99.4)	0.59 (0.25–1.41)
2	N1-2,ELI(−),AC(+)	42	83.0 (67.7–91.5)	0.77 (0.35–1.69)	97.6 (83.9–99.7)	0.88 (0.29–2.62)
3	N0,ELI(+),AC(−)	84	78.3 (67.8–85.7)	1.00	91.2 (82.4–95.7)	1.00
4	N1-2,ELI(+),AC(+)	29	69.0 (48.8–82.5)	1.36 (0.62–2.98)	89.7 (71.3–96.5)	1.81 (0.61–5.41)
5	N1-2,ELI(−),AC(−)	46	57.7 (41.9–70.6)	1.92 (1.03–3.57)	82.0 (67.1–90.5)	2.10 (0.88–5.01)
6	N1-2,ELI(+),AC(-)	69	55.9 (43.3–66.7)	2.36 (1.36–4.11)	79.5 (67.3–87.6)	2.64 (1.20–5.81)

N = nodal status; ELI = elastic laminal invasion; AC = adjuvant chemotherapy; RFS = recurrence-free survival; OS = overall survival.

(Table 4). The 5-year RFS for group 3 excluding those with pT4a disease (group 3′) was significantly worse than that for group 1′ (group 1 excluding those with pT4a disease; 81.1% vs 92.9%; $p = 0.003$). The RFS curve of group 3′ was similar to that of groups 2′ (group 2 excluding those with pT4a disease) and 4′ (group 4 excluding those with pT4a disease; group 3′ vs group 2′, $p = 0.61$; group 3′ vs group 4′, $p = 0.83$; Fig. 5A). The OS curve of group 3′ lay below that of groups 2′ and 4′ (group 3′ vs group 2′, $p = 0.41$; group 3′ vs group 4′, $p = 0.98$; Fig. 5B).

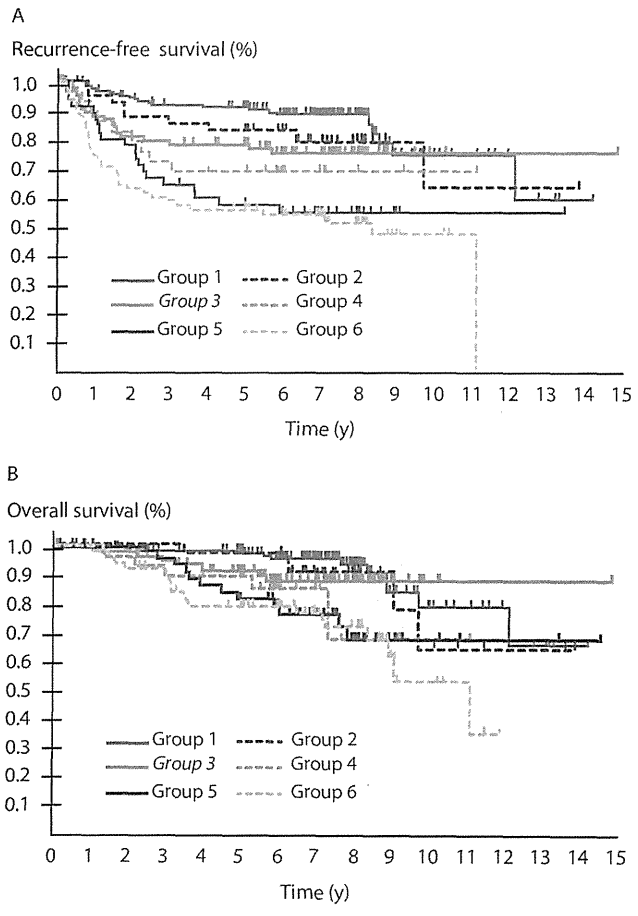

FIGURE 4. Kaplan-Meier curves depicting recurrence-free (A) and overall survival (B) of 6 groups of 436 patients who underwent primary resection for colon cancer, stratified according to elastic laminal invasion (ELI), lymph node metastasis, and adjuvant chemotherapy status. The green line represents group 3 (node negative, ELI positive, and no adjuvant chemotherapy).

DISCUSSION

ELI appears to influence outcome in patients with pT3 and pT4a CC. The RFS and OS of patients with ELI-negative NPCC (group 2) were better than those with ELI-positive NNCC (group 3). A similar trend was observed in previous reports based on the UICC 6th edition. Patients with stage IIIA (T1 to 2N1) disease had a better 5-year survival than those with stage IIA (T3N0) disease, and the Kaplan-Meier curve of patients with stage IIB (T4N0) disease lay approximately halfway between those of patients with stage IIIA and stage IIIB (T3-4N1) disease.[13,14] Whether the favorable outcome of patients with stage IIIA disease was because of limited tumor spread or adjuvant chemotherapy is unclear; these and our results show that some patients with stage II disease have a worse outcome than some with stage III disease.

Several studies have reported a variety of poor prognostic indicators in patients with stage II CC, including tumor necrosis,[15] perineural invasion,[15,16] male sex,[17] bowel obstruction,[17–19] tumor depth,[6,7,16–21] retrieval of less than 10 or 14 lymph nodes,[17,19] emergency presentation,[6] left colonic disease,[6] venous invasion,[20,21] lymphovascular invasion,[16,18,19,22] margin involvement,[20] differentiation pattern,[7] preoperative CEA level,[16] mucinous component of >50%,[18] tumor grade,[22] and tumor length.[22] Tumor depth and lymphovascular invasion have been identified most often. ELI status, which subdivides tumors invading beyond the muscularis propria, is also an indicator related to tumor depth. The "TNM Supplement: A Commentary on Uniform Use[23]" stated that the pT3 subclassification identified an extent of disease with a clinically relevant influence on outcome and could be used to determine the need for adjuvant chemotherapy.

There is a consensus that pT4 staging indicates a high risk of recurrence[24]; thus, the ELI status of patients other those with pT4a disease is also of great interest. The findings presented in Figure 5, from which patients with pT4a disease were excluded, show the poor prognosis of patients with ELI-positive NNCC with pT3 disease and indicate

TABLE 4. Comparison of 5-year RFS and OS of the 6 stratified groups excluding patients with pT4a disease

			RFS		OS	
Group		*n*	*5-y % (95% CI)*	*HR (95% CI)*	*5-y % (95% CI)*	*HR (95% CI)*
1′	N0,ELI(−),AC(−)	166	92.9 (88.9–97.0)	0.34 (0.16–0.73)	98.1 (95.9-NE)	0.46 (0.20–1.10)
2′	N1-2,ELI(−),AC(+)	41	82.6 (70.9–94.3)	0.79 (0.32–1.95)	97.5 (92.7-NE)	0.70 (0.23–2.09)
3′	N0,ELI(+),AC(−)	70	81.1 (71.9–90.4)	1.00	89.6 (82.3–96.9)	1.00
4′	N1-2,ELI(+),AC(+)	21	76.2 (58.0–94.4)	1.12 (0.40–3.12)	95.2 (86.1-NE)	0.81 (0.17–3.75)
5′	N1-2,ELI(−),AC(−)	46	59.8 (45.4–74.2)	2.09 (1.04–4.20)	82.0 (70.6–93.3)	1.65 (0.69–3.93)
6′	N1-2,ELI(+),AC(−)	49	62.5 (48.8–76.2)	2.21 (1.11–4.41)	80.1 (68.4–91.8)	2.04 (0.88–4.74)

N = nodal status; ELI = elastic laminal invasion; AC = adjuvant chemotherapy; RFS = recurrence-free survival; OS = overall survival; NE = not estimated.

that subclassification by ELI status allows valid conclusions to be made about outcome independent of tumor staging. The survival of patients with stage II CRC and pT3 deep tumor invasion (which represented tumors that had invaded beyond the PEL) has been reported to be equal to that of patients with stage II CRC and pT4 disease.[9] Therefore, a deeply invasive pT3 tumor, which fulfills the criteria for ELI used in this study, is a poor prognostic indicator.

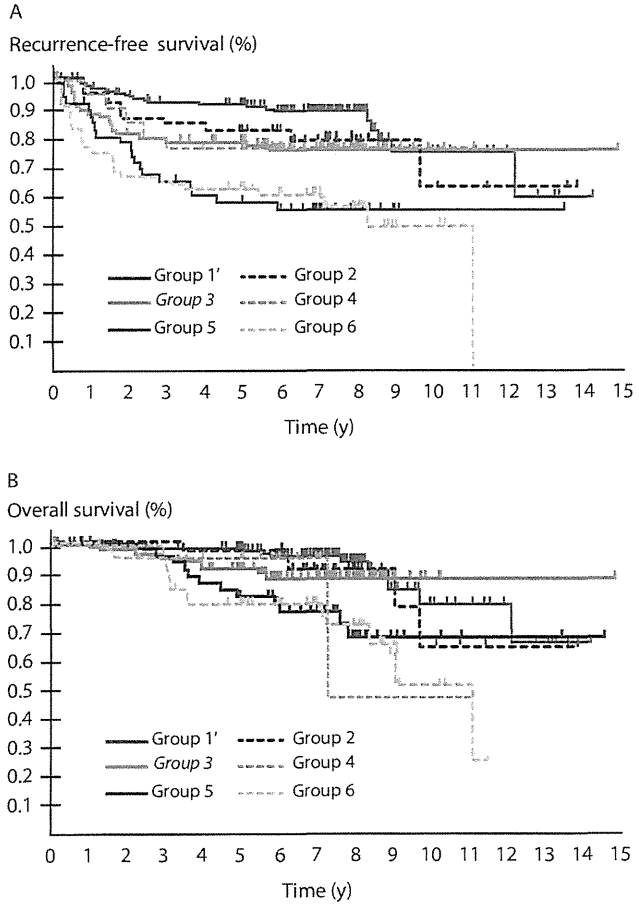

FIGURE 5. Kaplan-Meier curves depicting recurrence-free (A) and overall survival (B) of 6 groups of 393 patients who underwent primary resection for colon cancer, stratified according to elastic laminal invasion (ELI), lymph node metastasis, and adjuvant chemotherapy status after exclusion of those with pT4a disease. The green line represents group 3 excluding those with pT4a disease (group 3′; node negative, ELI positive, and no adjuvant chemotherapy).

Comparing the prognosis of stage II and III CC may help identify high-risk stage II patients. A small number of studies have reported the prognosis of stage II alongside that of stage III disease. The 5-year survival of patients with Dukes B CC determined to be at high risk by the Peterson index (43.3%) was worse than that of patients with Dukes C disease with a single lymph node metastasis (57.9%).[25] Patients with stage II CC and perineural invasion had significantly worse outcomes than stage III patients (5-year disease-free survival of 29% vs 56%; 5-year OS of 43% vs 67%).[26] This suggests that the Peterson index and perineural invasion may also be useful means of identifying a high-risk group for whom adjuvant chemotherapy might be recommended. Likewise, the RFS and OS of patients with ELI-positive NNCC were equivalent to those of patients with NPCC and pT3 or pT4a histology, corresponding with stage IIIB disease. Thus, ELI status appears to identify patients with high-risk stage II CC.

There is considerable variability in the incidence of serosal involvement in patients with Dukes stage B CC reported in previous studies,[27] which may reflect diagnostic difficulties.[28,29] One difficulty is that mesothelial cells are fragile, and the serosal surface may easily be disrupted during surgery and fixation. Another is that inflammatory and desmoplastic stromal reactions are often seen around the invasive tumor front. These problems can lead to underestimation of invasion because of the difficulty of demonstrating tumor cells on the peritoneal surface. In this regard, ELI may be advantageous because it is assessed from the inner surface of the serosa and is, therefore, not influenced by external trauma. Like vascular invasion, tumor spread might also be determined more objectively by routine elastica staining.[30,31]

ELI is sometimes affected by the tumor-associated inflammation around the invasive tumor front. In such cases, we speculate that the use of an estimated line and multiple histologic sections might provide a more precise and objective diagnosis. Nevertheless, we could not demonstrate ELI positivity in 2.3% of patients with pT4a disease. This is likely to be a consequence of marked in-

flammation at the tumor invasion front, making it impossible to determine ELI positivity in some patients with pT4a disease.

The prediction accuracy of our prognostic stratification is a limitation of our study, because we developed the risk group based only on the training set of 436 patients. A prospective study is needed to evaluate the validity and accuracy of our conclusions. Stratifying patients with CC into 6 groups based on 3 unfavorable factors led to an analysis of small subgroups that may not have been capable of detecting significant differences. Another limitation is that there was a wide range of H&E- and elastica-stained slides examined per case, because we did not adopt the protocol with a predefined the number of blocks and sections. This could cause bias in the ELI and pT4 rates.

The strength of our study was that not all of the patients with stage II CC routinely received adjuvant chemotherapy. If all of the patients predicted to have a poor outcome had received adjuvant chemotherapy, almost three quarters would have done so, making any comparison impossible.[32]

CONCLUSION

ELI status predicts prognosis in patients with pT3 and pT4a CC. Patients with ELI-positive NNCC have a worse outcome than those with ELI-negative histology and a prognosis similar to patients with stage III CC who received adjuvant chemotherapy. Therefore, although ELI positivity does not affect prognosis in patients with stage III CC receiving adjuvant chemotherapy, ELI is a strong prognostic factor to identify patients with high-risk stage II CC. Further prospective studies are needed to prove the reproducibility and validity of our findings.

REFERENCES

1. Jemal A, Bray F, Center MM, Ferlay J, Ward E, Forman D. Global cancer statistics. *CA Cancer J Clin.* 2011;61:69–90.
2. Siegel R, Naishadham D, Jemal A. Cancer statistics, 2012. *CA Cancer J Clin.* 2012;62:10–29.
3. Ferlay J, Parkin DM, Steliarova-Foucher E. Estimates of cancer incidence and mortality in Europe in 2008. *Eur J Cancer.* 2010;46:765–781.
4. Center for Cancer Control and Information Services, National Cancer Center, Japan. Latest cancer statistics. http://ganjoho.jp/public/statistics/pub/statistics01.html. Accessed November 20, 2012.
5. Sobin LH, Gospodarowicz MK, Wittekind C. *TNM Classification of Malignant Tumors.* 7th ed. West Sussex, United Kingdom: Wiley-Blackwell; 2009.
6. Merkel S, Wein A, Günther K, Papadopoulos T, Hohenberger W, Hermanek P. High-risk groups of patients with stage II colon carcinoma. *Cancer.* 2001;92:1435–1443.
7. Cianchi F, Messerini L, Comin CE, et al. Pathologic determinants of survival after resection of T3N0 (Stage IIA) colorectal cancer: proposal for a new prognostic model. *Dis Colon Rectum.* 2007;50:1332–1341.
8. Pollheimer MJ, Kornprat P, Pollheimer VS, et al. Clinical significance of pT sub-classification in surgical pathology of colorectal cancer. *Int J Colorectal Dis.* 2010;25:187–196.
9. Shinto E, Ueno H, Hashiguchi Y, et al. The subserosal elastic lamina: an anatomic landmark for stratifying pT3 colorectal cancer. *Dis Colon Rectum.* 2004;47:467–473.
10. Kojima M, Nakajima K, Ishii G, Saito N, Ochiai A. Peritoneal elastic laminal invasion of colorectal cancer: the diagnostic utility and clinicopathologic relationship. *Am J Surg Pathol.* 2010;34:1351–1360.
11. Puchtler H, Sweat F. Commercial resorcin-fuchsin as a stain for elastic fibers. *Stain Technol.* 1960;35:347–348.
12. Furnival GM, Wilson, R.W. Regression by leaps and bounds. *Technometrics.* 1974;16:499–511.
13. O'Connell JB, Maggard MA, Ko CY. Colon cancer survival rates with the new American Joint Committee on Cancer sixth edition staging. *J Natl Cancer Inst.* 2004;96:1420–1425.
14. Gunderson LL, Jessup JM, Sargent DJ, Greene FL, Stewart AK. Revised TN categorization for colon cancer based on national survival outcomes data. *J Clin Oncol.* 2010;28:264–271.
15. Mulcahy HE, Toner M, Patchett SE, Daly L, O'Donoghue DP. Identifying stage B colorectal cancer patients at high risk of tumor recurrence and death. *Dis Colon Rectum.* 1997;40:326–331.
16. Quah HM, Chou JF, Gonen M, et al. Identification of patients with high-risk stage II colon cancer for adjuvant therapy. *Dis Colon Rectum.* 2008;51:503–507.
17. Burdy G, Panis Y, Alves A, Nemeth J, Lavergne-Slove A, Valleur P. Identifying patients with T3-T4 node-negative colon cancer at high risk of recurrence. *Dis Colon Rectum.* 2001;44:1682–1688.
18. Lin CC, Lin JK, Chang SC, et al. Is adjuvant chemotherapy beneficial to high risk stage II colon cancer? Analysis in a single institute. *Int J Colorectal Dis.* 2009;24:665–676.
19. Koebrugge B, Vogelaar FJ, Lips DJ, et al. The number of high-risk factors is related to outcome in stage II colonic cancer patients. *Eur J Surg Oncol.* 2011;37:964–970.
20. Petersen VC, Baxter KJ, Love SB, Shepherd NA. Identification of objective pathological prognostic determinants and models of prognosis in Dukes' B colon cancer. *Gut.* 2002;51:65–69.
21. Morris M, Platell C, de Boer B, McCaul K, Iacopetta B. Population-based study of prognostic factors in stage II colonic cancer. *Br J Surg.* 2006;93:866–871.
22. Gertler R, Rosenberg R, Schuster T, Friess H. Defining a high-risk subgroup with colon cancer stages I and II for possible adjuvant therapy. *Eur J Cancer.* 2009;45:2992–2999.
23. Wittekind C, Compton CC, Brierley J. *TNM Supplement: A Commentary on Uniform Use.* 4th ed. West Sussex, United Kingdom: Wiley-Blackwell; 2012.
24. Shepherd NA, Baxter KJ, Love SB. The prognostic importance of peritoneal involvement in colonic cancer: a prospective evaluation. *Gastroenterology.* 1997;112:1096–1102.
25. Morris EJ, Maughan NJ, Forman D, Quirke P. Who to treat with adjuvant therapy in Dukes B/stage II colorectal cancer? The need for high quality pathology. *Gut.* 2007;56:1419–1425.
26. Liebig C, Ayala G, Wilks J, et al. Perineural invasion is an independent predictor of outcome in colorectal cancer. *J Clin Oncol.* 2009;27:5131–5137.

27. Stewart CJ, Morris M, de Boer B, Iacopetta B. Identification of serosal invasion and extramural venous invasion on review of Dukes' stage B colonic carcinomas and correlation with survival. *Histopathology.* 2007;51:372–378.
28. Kojima M, Yokota M, Saito N, Nomura S, Ochiai A. Elastic laminal invasion in colon cancer: diagnostic utility and histological features. *Front Oncol.* 2012;2:179.
29. Puppa G, Shepherd NA, Sheahan K, Stewart CJ. Peritoneal elastic lamina invasion in colorectal cancer: the answer to a controversial area of pathology? *Am J Surg Pathol.* 2011;35:465–468.
30. Kirsch R, Messenger DE, Riddell RH, et al. Venous invasion in colorectal cancer: impact of an elastin stain on detection and interobserver agreement among gastrointestinal and nongastrointestinal pathologists. *Am J Surg Pathol.* 2013;37:200–210.
31. Abdulkader M, Abdulla K, Rakha E, Kaye P. Routine elastic staining assists detection of vascular invasion in colorectal cancer. *Histopathology.* 2006;49:487–492.
32. O'Connor ES, Greenblatt DY, LoConte NK, et al. Adjuvant chemotherapy for stage II colon cancer with poor prognostic features. *J Clin Oncol.* 2011;29:3381–3388.